RAPID COMMUNICATIONS

PHYSICAL REVIEW B VOLUME 50, NUMBER 7 15 AUGUST 1994-I

Nucleation with a critical cluster size of zero: Submonolayer Fe inclusions in Cu(100)

David D. Chambliss and Kevin E. Johnson*

IBM Research Division, Almaden Research Center, 650 Harry Road, San Jose, California 95120

(Received 12 May 1994)

A single-atom nucleation model is studied in which monomers randomly and irreversibly react with the substrate to become immobile and act as growth nuclei. The reaction kinetics, of first order in monomer density, yields a cluster size distribution that is insensitive to deposition rate and is a decreasing function of cluster size. This matches the experimental behavior of submonolayer Fe inclusions formed by deposition onto room-temperature Cu(100) and observed with the scanning tunneling microscope.

The scaling properties of island nucleation and growth have been recognized as a tool for extracting characteristics of atomic behavior, such as activation barriers for diffusion, from scanning tunneling microscope (STM) images of epitaxial growth.[1] Recent simulations and rate-equation analyses[2–5] have extended the well-established field of the nonequilibrium kinetics of epitaxial growth,[6] with an emphasis on the conventional assumption that two or more mobile adatoms must combine to form an immobile nucleus for island aggregation.

In this paper we present two related results. First we derive the properties of "single-atom nucleation," a category of diffusion-mediated nucleation and growth, in which the formation of a stable cluster nucleus involves only one mobile monomer. The properties include the persistent presence of small clusters and an insensitivity of the size and number of clusters to the deposition flux. Second, we apply this analysis to STM results on the statistics of Fe inclusions formed in the Cu(100) surface by room-temperature deposition.[7–9]

We use mean-field rate equations to describe the irreversible nucleation and growth of immobile clusters from a two-dimensional gas of monomers, which are deposited at a rate F. Quantities are expressed in surface lattice units unless otherwise stated. Given a number density n of monomers with diffusivity (equal to the hopping rate) D, the irreversible addition of monomers to immobile clusters causes the density N_s of clusters of size s to evolve by

$$\frac{dN_s}{dt}=D(\sigma_{s-1}N_{s-1}-\sigma_s N_s)n. \tag{1}$$

Here σ_s is a capture number[6] which in general depends not only on s but also on the number of clusters and possibly their size distribution. A common approximation is $\sigma_s \propto s^p$ for some p. We will consider the case $p=0$ (the point-cluster approximation), which is accurate in the low-coverage limit, as well as $p>0$ which is appropriate for closer-spaced islands in which capture probability depends on the perimeter of clusters.[10]

Equation (1) applies for $s>i+1$ where i is the critical cluster size: clusters with $s\leq i$ are either mobile or unstable against reevaporation. In the usual model, all monomers are mobile and dimers are stable and immobile, so $i=1$, $N_1=0$, and the equation for $s=2$ differs from Eq. (1) by including the quadratic nucleation term $(D\sigma_1 n^2)$ in place of $(D\sigma_{s-1}N_{s-1}n)$. We consider here instead the case where mobile monomers can react with the surface to become immobile. For Fe adatoms on Cu(100) this reaction is apparently an atomic exchange with a surface atom [like those first observed for Pt on Pt(100) (Ref. 11)], producing a Cu adatom and an Fe atom embedded in the surface[7,8,12] [Fig. 1(a)]. For this assumption the critical cluster size is $i=0$ and Eq. (1) applies for all $s>1$. The rate at which monomers become immobile (and clusters are nucleated) can be written as $D\sigma_0 N_0 n$, where N_0 is the density of sites available for exchange and σ_0 is the probability of reacting per hop in a single-step random walk. With this notation, Eq. (1) applies *for all* s. (We assume n is small enough that direct formation of multiatom clusters can be neglected.) If clusters are energetically favored one has $\sigma_0<\sigma_s$ for all s. In our experiments, strong Fe-Fe bonding may lower the activation barrier for exchange at the edge of an existing cluster [Fig. 1(b)] and thus increase σ_s. Cluster growth is kinetically possible if $\sigma_0 \ll 1$. We might have $\sigma_s \ll 1$ within these conditions, because cluster growth too may have an activation barrier.

Mobile monomers arrive randomly, and are lost by absorption:

$$\frac{dn}{dt}=F-D\left(\sum_{s\geq 0}\sigma_s N_s\right)n=F-D(\sigma_0 N_0+\bar{\sigma}N)n, \tag{2}$$

where $N=\Sigma_{s\geq 1}N_s$ is the total cluster density and an average capture number $\bar{\sigma}=(\Sigma_{s\geq 1}\sigma_s N_s)/N$ is defined. Let $\theta=\int F dt-n$, the coverage of monomers aggregated in clusters. Then $d\theta/dt=D(\sigma_0 N_0+\bar{\sigma}N)n$ and

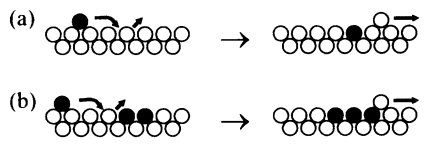

FIG. 1. Fe inclusion formation in Cu(100) by atomic exchange. Schematic cross section is shown. (a) Nucleation. Fe-Cu exchange converts mobile Fe adatom to immobile embedded Fe atom plus mobile Cu adatom (which adheres to step elsewhere). (b) Growth. Subsequent exchange of Fe atoms at perimeter of inclusion is energetically more favorable because positive Fe-Cu heat of mixing favors Fe-Fe bonding.

 © 1994 The American Physical Society

$$\frac{dN_s}{d\theta}=\frac{dN_s/dt}{d\theta/dt}=\frac{\sigma_{s-1}N_{s-1}-\sigma_sN_s}{\sigma_0N_0+\tilde{\sigma}N} \quad \text{for } s>0. \tag{3}$$

The evolution of $N_s(\theta)$ as determined by Eq. (3) is independent of F and D, and if the time between deposition and measurement is $\gg(DN)^{-1}$, all deposited atoms have time to reach clusters and we can identify θ with the deposited dose Θ. The dependence of N_s only on Θ is the most important property of this nucleation process. It is a direct consequence of our choice to omit terms from the rate equation that embody interaction between mobile monomers. It applies for any (possibly θ-dependent) form of σ_s, for F and D that may vary in time, and for modified equations including terms to account for direct impingement of atoms on cluster surfaces and perimeters, all provided that σ_s and the added terms involve no adatom-adatom interactions and σ_s is not explicitly time dependent. Of course if (F/D) is large enough ($\sim\sigma_0^2$), two-atom nucleation cannot be neglected and these equations and conclusions no longer apply.

We note that in Eq. (3) only the *relative* values of σ_s affect the final distribution. A uniform rescaling of σ_s is equivalent to a change in D or in time scale.

For $\theta\ll 1$ it is reasonable to approximate N_0 as a constant $\equiv 1$. While clusters make sites unavailable for monomer reaction with the surface, the correction term is small, comparable to the terms already omitted for direct impingement of atoms onto clusters. We also assume σ_s depends only on s, not on coverage. Then with initial conditions $N_s|_{\theta=0}=0$ for $s>0$, it follows by induction on s that N_s is a monotonically increasing function of θ, asymptotically approaching σ_0/σ_s, and that $\sigma_0N_0>\sigma_1N_1>\sigma_2N_2>\cdots$. Thus, in contrast to two-atom nucleation [Fig. 2(c)], this process yields no peak (except in the unexpected situation that σ_s is nonmonotonic in s, i.e., a larger island may have a smaller capture number). These properties are illustrated in Fig. 2 for numerical solutions to the rate equations.

For the point-cluster case ($p=0$, so $\sigma_s=1$ for all $s>0$), there is an exact solution to Eq. (3): $N=\sigma_0(\sqrt{1+2\theta/\sigma_0}-1)\approx\sqrt{2\sigma_0\theta}$ for $\theta\gg\sigma_0$ and, with $\eta=N/\sigma_0$,

$$N_s=\sigma_0\left(1-e^{-\eta}\left[1+\eta+\cdots+\frac{\eta^{s-1}}{(s-1)!}\right]\right). \tag{4}$$

The asymptotic approach $N_s\to\sigma_0$ is evident in Eq. (4). For $p>0$ one gets $N\sim\theta^\eta$ with $\eta=1-1/(2-p)$ when $\theta\gg\sigma_0$.

These predictions are compared with results of STM experiments on the growth of Fe on Cu(100) at room temperature. These experiments[7,8,12] showed that, for $\Theta<0.2$, most Fe atoms are incorporated into planar clusters in the topmost Cu layer ("inclusions"), as shown in Fig. 1. Deposition beyond $\Theta=0.2$ leads to enhanced nucleation of first-layer islands atop the inclusions;[13] we deal here with low coverages for which few islands are found. The visibility of Fe inclusions in STM images is sensitive to tip condition and tunnel junction voltage. They appear as shallow depressions or bumps, or in exceptional cases (<10% of images) as holes > 1 Å deep with clear boundaries (Fig. 3). These features are identified as Fe clusters by their behavior when Fe coverage and substrate temperature are varied. Another group has observed "Fe features"[14] like our typical images of Fe inclusions, but has not reproduced the more unusual deep-hole

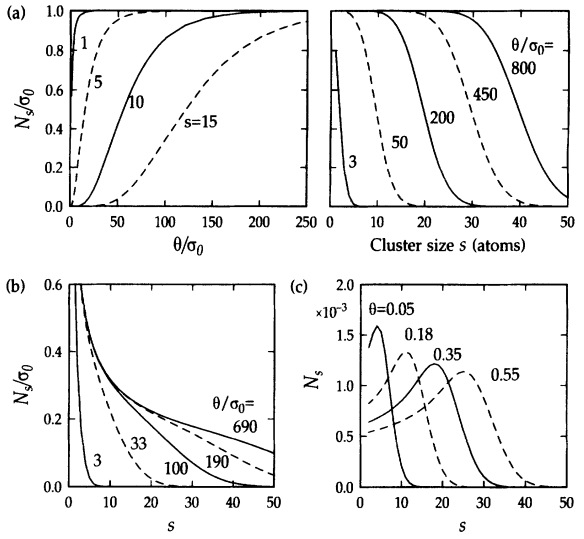

FIG. 2. Properties of one-atom-nucleation computed from rate equations. (a) N_s for point-cluster model ($\sigma_s=1$). N_s for each s approaches σ_0 with increasing θ. At fixed θ, N_s is nearly constant up to cutoff at $s=(\theta/\sigma_0)^{1/2}$. N_s scales exactly linearly with σ_0. (b) N_s for $p=1/2$ model ($\sigma_s=s^{1/2}$). Similar qualitative behavior is seen as for (a), with different limit $\sigma_0 s^{-1/2}$. Cutoff of size distribution is less abrupt than in (a). (c) N_s for two-atom nucleation, $\sigma_s=1$, computed with $F/D=1.5\times10^{-5}$ ($D=800$ s^{-1}). Curves display clear peaks.

appearance we have obtained for each of our low-coverage samples. We have extracted the total inclusion populations [Figs. 4(a) and 4(b)] and their size distribution [Figs. 4(c) and 4(d)] from "deep-hole" images.

The exchange of Fe adatoms with Cu is favored by the higher surface energy of Fe than Cu. The positive enthalpy of mixing for Fe in Cu favors Fe-Fe bonds over Fe-Cu bonds and drives Fe clustering. Our model is that an Fe adatom moves by hopping diffusion before exchange, and is more likely to exchange as a neighbor of another embedded Fe atom [Fig. 1(b)]. An alternative model is that Fe atoms exchange with Cu immediately but remain mobile enough to aggregate. STM results appear to show single embedded Fe atoms that are immobile on a time scale >100 s, but this is not conclusive. Cluster statistics, however, can indicate that aggregation occurs via preexchange motion. If embedded atoms were mobile, cluster formation would be mathematically equivalent to island formation from adatoms, with $i>0$ and corresponding size distribution and scaling of cluster densities.

The number of inclusions and their sizes agree with the predictions for one-atom nucleation. They are rate independent: a 12× change in F causes no change in the number density of inclusions [Fig. 4(a)]. The weak variation with Θ is consistent with both $p=0$ (for which $N\sim\Theta^{1/2}$) and $p=1/2$ ($N\sim\Theta^{1/3}$). The size distributions for two samples with different values of F and Θ agree reasonably well with computed curves for the cases $p=0,1/4,1/2$, using the same values of σ_0/σ_1 for both samples (0.0007, 0.0009, and 0.0014, respectively) [Figs. 4(c) and 4(d)]. The agreement appears better for $p=0$ in the lower-coverage data of (d), and

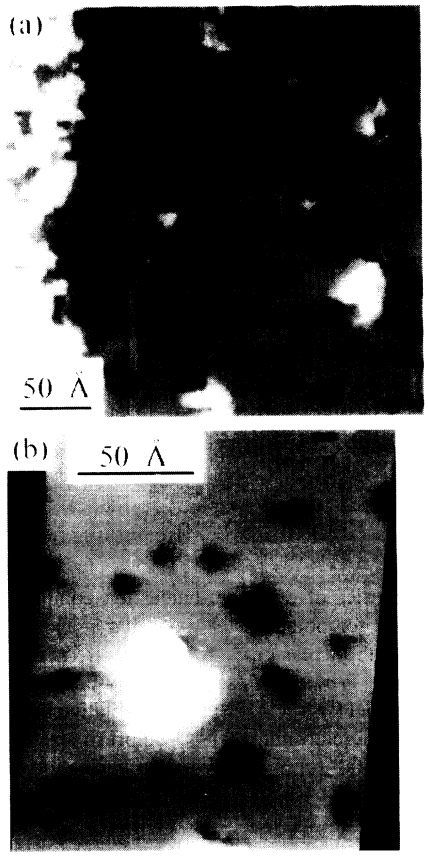

FIG. 3. STM images of Fe clusters in Cu(100) surface. (a) Coverage $\theta=0.11$ at rate $F=0.012$ s^{-1}, imaged using sample bias $V_S=-1.9$ V and current 1 nA. (b) $\theta=0.06$, $F=0.001$ s^{-1}, $V_S=-0.7$ V, $I_{tun}=1$ nA. Fe inclusions appear dark, as if below surface level, as artifact of STM tip behavior. Tips sensitive to Fe-Cu difference typically do not yield sharpest images of monoatomic steps and islands. Separate atoms are not resolved in multiatom clusters. Note different length scales for (a) and (b).

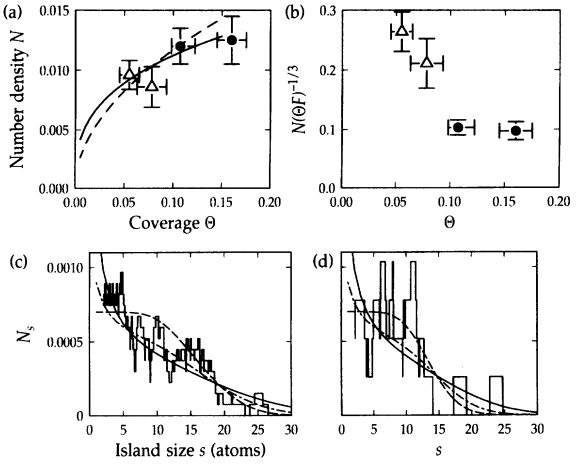

FIG. 4. Comparison of experimental inclusion statistics with one-atom nucleation model. (a) Total inclusion density N vs Fe deposition for different samples and rates $F=0.012$ s^{-1} (●) and $F=0.001$ s^{-1} (△). Curves display power-law behavior expected for point-cluster ($p=0$) model ($N \propto \theta^{1/2}$, dashed) and for $p=1/2$ model ($N \propto \theta^{1/3}$, solid). For highest coverage shown, N may be underestimated because first-layer islands preferentially cover inclusions, and inclusion coverage θ is less than total coverage Θ because of aggregation into layer-1 islands. (b) Data of (a) scaled as for conventional nucleation with $i=1$, $p=0$. If that model were valid here, the data would lie on a horizontal line. (c) Size distribution of inclusions for data of Fig. 3(a). Curves represent solutions to Eq. (3) at $\theta=0.11$, for $p=0$ with $\sigma_0/\sigma_1=0.0007$ (dashed), $p=1/2$, $\sigma_0/\sigma_1=0.0014$ (solid), and $p=1/4$, $\sigma_0/\sigma_1=0.0010$ (dot-dash). (d) Size distribution for data of Fig. 3(b). Curves are as in (b) with same σ_0/σ_1 values but $\theta=0.06$. Note that vertical scale in (c) and (d) is the same despite a 12× difference in deposition rate.

for $p=1/4$ or $1/2$ in (c), possibly because σ_s should be size independent (i.e., $p\approx 0$) for low Θ but should approach linearity in cluster diameter for high enough Θ.[10] Because the form $\sigma_s \propto s^p$ is inadequate we do not compute a best-fit value of p from the data.

The experimental results are inconsistent with the $N\sim(F/D)^{1/3}\Theta^{1/3}$ scaling for two-atom nucleation of point clusters[4] [Fig. 4(b)]; for $i>1$ or $p>0$ the disagreement is worse. Furthermore, neither Fig. 4(c) nor 4(d) shows the clear peak expected for multiatom nucleation [Fig. 2(d)]. Therefore the clusters do not form by aggregation of mobile embedded atoms *during* deposition. Aggregation *after* deposition, but before data acquisition, is conceivable for our time scales (100 s vs 10^4 s). In the limit of slow diffusion the final configuration would be independent of F, but N scales as $\Theta^{(i+1)/2}$. For example, when $F=0$ the rate equations for $i=1$ are invariant under the scaling $n(t)\mapsto\beta n(\beta t)$ and $N_s(t)\mapsto\beta N_s(\beta t)$. Since $n(t)$ and $N_s(t)$ scale identically, the final distribution $N_s(\infty)$ varies linearly with the initial conditions $n(0)=\Theta$, which is inconsistent with the data. In summary the data rule out $i>0$ for aggregation during or after deposition. Another model with rate-independent results would be nucleation by defects present before deposition. The equal age of clusters in that model, however, would imply clusters of near uniform size (i.e., a peaked size distribution) since size variations would arise only from shot noise and differences in cluster spacing.

The experiments yield $0.0007\leq\sigma_0/\sigma_1\leq 0.0014$, depending on the choice of exponent p. This is the ratio of the exchange probability for an Fe atom on clean Cu to its probability beside an Fe inclusion. This could result from an energy barrier difference of $\Delta E_{\text{exch,Cu}}-\Delta E_{\text{exch,Fe}} = -kT\ln(\sigma_0/\sigma_1)=180\pm 10$ meV; one expects these processes to have similar prefactors. The final states for the two cases differ in energy because inclusion growth creates Fe-Fe bonds. For comparison, average bond strengths computed from surface energies and enthalpy of mixing yield the estimate $E_{\text{Fe-Fe}}-E_{\text{Fe-Cu}}\sim 90$ meV per bond.[15] We can also place an upper bound on σ_0, since clustering presumably involves only nearest-neighbor bonding, which limits σ_s to the number of nearest-neighbor sites (i.e., $\sigma_1\leq 4$). Thus $\sigma_0<0.005$ expresses the ratio between rates of exchange and hopping diffusion. This may reflect not only a difference in energy barrier but also different prefactors for (two-atom) exchange and (one-atom) hopping. It would be valuable to compute these energies accurately using *ab initio* methods.

The properties of single-atom nucleation presented here have proved useful for understanding the microscopic mechanism of Fe inclusion formation on Cu(100). For many

other epitaxial systems, reaction with the substrate is a significant concern, and if such reaction nucleates cluster growth above or below the surface, the characteristic cluster statistics of single-atom nucleation will be observable. Growth of two-component X-Y films can also yield similar kinetics, if one component X by itself is slow to form stable clusters (e.g., the critical cluster size is large), so the dominant nucleation step involves one type-Y atom reacting with X. Preliminary STM results suggest that Co-Ag codeposition on Mo(110) may behave this way, with X=Ag and Y=Co. While the broad cluster size distribution of single-atom nucleation makes it readily identifiable, it is undesirable in many situations where uniformity is preferred. Thus the study of this nucleation mode can be valuable not just for understanding surface-adatom interactions but for obtaining desirable characteristics in film growth.

We are grateful to A. Zangwill and J. Amar for helpful discussions.

*Present address: Department of Chemistry, Pacific University, Forest Grove, Oregon 97116.

[1] J. A. Stroscio and D. T. Pierce, Phys. Rev. B **49**, 8522 (1994).
[2] M. C. Bartelt and J. W. Evans, Phys. Rev. B **46**, 12 675 (1992).
[3] J. G. Amar, F. Family, and P.-M. Lam, in *Mechanisms of Thin Film Evolution*, MRS Symposia Proceedings No. 317 (Materials Research Society, Pittsburgh, 1994), pp. 167–173.
[4] J. G. Amar, F. Family, and P.-M. Lam, Phys. Rev. B (to be published).
[5] C. Ratsch, A. Zangwill, P. Šmilauer, and D. D. Vvedensky, Phys. Rev. Lett. **72**, 3194 (1994).
[6] J. A. Venables, G. D. T. Spiller, and M. Hanbücken, Rep. Prog. Phys. **47**, 399 (1984).
[7] D. D. Chambliss, R. J. Wilson, and S. Chiang, J. Vac. Sci. Technol. B **10**, 1993 (1992).
[8] K. E. Johnson, D. D. Chambliss, R. J. Wilson, and S. Chiang, J. Vac. Sci. Technol. A **11**, 1654 (1993).
[9] T. Detzel, N. Memmel, and T. Fauster, Surf. Sci. **293**, 227 (1993).
[10] G. S. Bales and D. C. Chrzan, Phys. Rev. B (to be published).
[11] G. L. Kellogg and P. J. Feibelman, Phys. Rev. Lett. **64**, 3143 (1990).
[12] D. D. Chambliss *et al.*, in *Magnetic Ultrathin Films: Multilayers and Surfaces, Interfaces and Characterization*, edited by B. Jonker *et al.* (Materials Research Society, Pittsburgh, 1993), pp. 713–722.
[13] K. E. Johnson, D. D. Chambliss, R. J. Wilson, and S. Chiang, Surf. Sci. Lett. **313**, L811 (1994).
[14] A. Brodde and H. Neddermeyer, Surf. Sci. **287/288**, 988 (1993).
[15] D. D. Chambliss and K. E. Johnson (unpublished).

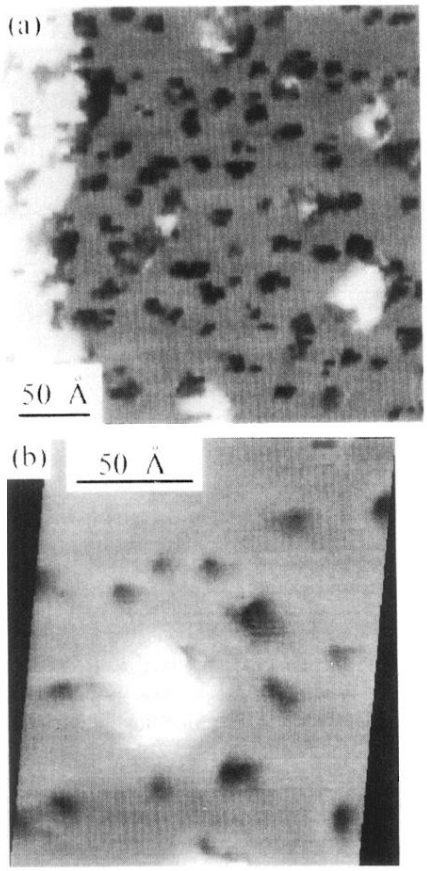

FIG. 3. STM images of Fe clusters in Cu(100) surface. (a) Coverage $\theta = 0.11$ at rate $F = 0.012\ s^{-1}$, imaged using sample bias $V_S = -1.9$ V and current 1 nA. (b) $\theta = 0.06$, $F = 0.001\ s^{-1}$, $V_S = -0.7$ V, $I_{tun} = 1$ nA. Fe inclusions appear dark, as if below surface level, as artifact of STM tip behavior. Tips sensitive to Fe-Cu difference typically do not yield sharpest images of monoatomic steps and islands. Separate atoms are not resolved in multiatom clusters. Note different length scales for (a) and (b).